

1-1-2023

## Closing the shell: Gas-phase solvation of halides by 1,3-butadiene

Peter D. Watson

Christian T. Haakansson

Hayden T. Robinson

Timothy R. Corkish

James Brookes

*See next page for additional authors*

Follow this and additional works at: <https://ro.ecu.edu.au/ecuworks2022-2026>

 Part of the [Chemistry Commons](#)

---

[10.1002/chem.202203570](https://doi.org/10.1002/chem.202203570)

Watson, P. D., Haakansson, C. T., Robinson, H. T., Corkish, T. R., Brookes, J. R., McKinley, A. J., & Wild, D. A. (2023). Closing the Shell: Gas-phase solvation of halides by 1,3-butadiene. *Chemistry—A European Journal*. Advance online publication. <https://doi.org/10.1002/chem.202203570>

This Journal Article is posted at Research Online.  
<https://ro.ecu.edu.au/ecuworks2022-2026/2450>

---

**Authors**

Peter D. Watson, Christian T. Haakansson, Hayden T. Robinson, Timothy R. Corkish, James Brookes, Allan J. McKinley, and Duncan A. Wild

# Excellence in Chemistry Research

## Announcing our new flagship journal

- Gold Open Access
- Publishing charges waived
- Preprints welcome
- Edited by active scientists



## Meet the Editors of *ChemistryEurope*



**Luisa De Cola**

Università degli Studi  
di Milano Statale, Italy



**Ive Hermans**

University of  
Wisconsin-Madison, USA



**Ken Tanaka**

Tokyo Institute of  
Technology, Japan

# Closing the Shell: Gas-Phase Solvation of Halides by 1,3-Butadiene

Peter D. Watson,<sup>[a, b]</sup> Christian T. Haakansson,<sup>[a]</sup> Hayden T. Robinson,<sup>[a]</sup> Timothy R. Corkish,<sup>[a]</sup> James R. Brookes,<sup>[a]</sup> Allan J. McKinley,<sup>[a]</sup> and Duncan A. Wild<sup>\*[a, c]</sup>

**Abstract:** Gas-phase solvation of halides by 1,3-butadiene has been studied via a combination of photoelectron spectroscopy and density functional theory. Photoelectron spectra for  $X^{\cdot-} \cdots (C_4H_6)_n$  ( $X = Cl, Br, I$  where  $n = 1-3, 1-3$  and  $1-7$  respectively) are presented. For all complexes, the calculated structures indicate that butadiene is bound in a bidentate fashion through hydrogen-bonding, with the chloride complex showing the greatest degree of stabilisation of the

internal C–C rotation of *cis*-butadiene. In both  $Cl^-$  and  $Br^-$  complexes, the first solvation shell is shown to be at least  $n = 4$  from the vertical detachment energies (VDEs), however for  $I^-$ , increases in the VDE may suggest a metastable, partially filled, first solvation shell for  $n = 4$  and a complete shell at  $n = 6$ . These results have implications for gas-phase clustering in atmospheric and extraterrestrial environments.

## Introduction

In recent years, much interest has been generated as to the formation of large carbon aggregations from monomer units in the interstellar medium (ISM). Unlike smaller unsaturated hydrocarbons (i.e. propene), direct observation of 1,3-butadiene has not been reported, but as 1,3-butadiene represents a potential important intermediate in the formation of larger carbon units (Equations 1a–1c), it still remains of astrochemical interest. Currently, butadiene is believed to form in extraterrestrial ices, particularly methane ices with the addition of monomer radical species.<sup>[1]</sup> As the degree of unsaturation is the property of butadiene that supports this hydrocarbon growth, a number of

studies have investigated the reaction of radical species with butadiene as pathways within larger astrochemical processes. The addition reaction of the ethynyl radical ( $\cdot C_2H$ ) yields the formation of benzene, with similar mechanisms proposed for the formation of nitrogen containing heterocycles and substituted naphthalenes.<sup>[2]</sup> These include reactions with cyano ( $\cdot CN$ ), phenyl ( $\cdot C_6H_5$ ) and *meta*-tolyl ( $\cdot C_7H_7$ ) radicals respectively.<sup>[3–5]</sup>



Terrestrially, butadiene is a notable product of combustion reactions and occurs from both anthropogenic sources in the burning of fuel mixtures as well as natural sources such as from forest fires.<sup>[6,7]</sup> In combustion reactions, one such mechanism for butadiene formation is from the decomposition of the  $C_9H_{12}$  diradical which occurs on a picosecond timescale.<sup>[6]</sup> Once formed, it undergoes similar radical chemistry to produce larger carbon aggregates believed to be precursors to soot formation.<sup>[8]</sup>

Atmospherically, brominated butadiene radicals activate the oxidation of butadiene with a weaker Br–C bond forming a good leaving group and addition site on the neighbouring carbon, as illustrated in Equation 2.



The rate constant for this reaction is then  $4.7 \times 10^{-13} \text{ cm}^{-3} \text{ molecule}^{-1} \text{ s}^{-1}$  at 298 K and 700 Torr.<sup>[9]</sup> For the chlorinated analogue, the stronger Cl–H interaction is believed to favour hydrogen abstraction reactions and the formation of corresponding radicals. The experimentally measured rate constant

[a] P. D. Watson, C. T. Haakansson, H. T. Robinson, T. R. Corkish, J. R. Brookes, Prof. A. J. McKinley, Dr. D. A. Wild  
School of Molecular Sciences  
The University of Western Australia  
35 Stirling Hwy, Crawley,  
Australia, 6009  
E-mail: duncan.wild@uwa.edu.au

[b] P. D. Watson  
Department of Chemistry,  
Physical and Theoretical Chemistry Laboratory  
University of Oxford  
South Parks Road, Oxford,  
United Kingdom, OX1 3QZ

[c] Dr. D. A. Wild  
School of Science  
Edith Cowan University  
Joondalup, Australia, 6027  
E-mail: d.wild@ecu.edu.au

Supporting information for this article is available on the WWW under <https://doi.org/10.1002/chem.202203570>

© 2023 The Authors. Chemistry - A European Journal published by Wiley-VCH GmbH. This is an open access article under the terms of the Creative Commons Attribution Non-Commercial NoDerivs License, which permits use and distribution in any medium, provided the original work is properly cited, the use is non-commercial and no modifications or adaptations are made.

for the reaction of chlorine atoms with butadiene here is  $3.31 \times 10^{-10} \text{ cm}^{-3} \text{ molecule}^{-1} \text{ s}^{-1}$ .<sup>[7]</sup> The structure of these intermediates involve the insertion of the halogen into the C=C bond, bonding with the terminal carbon.

Despite the importance of butadiene radical interactions in both atmospheric and extraterrestrial environments, there are few studies investigating the geometric and electronic structure of these complexes. Halide-butadiene complexes represent a good analogue for these systems, as anion complexes typically feature bonding motifs that differ to their neutral counterparts, allowing for spectroscopic investigation into regions of the neutral potential energy surface other than local minima. Additionally, as the halides represent simple analogues for a number of anion-molecule interactions, investigating the structure of these complexes may provide insight into the radical chemistry present in extraterrestrial environments. While these reactions may be modelled as well behaved bimolecular systems, the role of gas-phase solvation may also be important in their structure and reactivity.<sup>[10]</sup>

Beyond these contexts, the study of halide-butadiene systems may also provide insight into the pre-reaction van der Waals (vdW) complexes of important synthetic reactions, namely the Diels-Alder reaction, pericyclic reactions of dienes that form a suite of ring-containing structures.<sup>[11]</sup> The stereoselectivity of these products is governed by the structure of the pre-reaction adduct prior to the concerted ring-closing mechanism, and by substituting the dieneophile for a model anion may provide insight into these reactions.<sup>[12]</sup>

This work investigates a number of solvated halide-butadiene complexes using a combination of theoretical methods and anion photoelectron spectroscopy. The electronic structure of solvated systems is approached by the electronic stabilisation energy of each successive solvated butadiene molecule (denoted  $E_{\text{solv}}$ ). From these energies and the binding motifs present, the structure of larger solvated species may be inferred.

## Results and Discussion

### Computational Results

Anion and neutral structures have been optimised using the DSD-PBEP86-D3BJ functional for the halide/halogen-butadiene complexes (Figure 1). For the anion complexes the minima are the 1, 2 and 4*trans* conformers, with the most stable for all three halides being the 2*trans*. This conformer features the halide bound to the hydrogen atoms attached to carbons 1 and 3 in the butadiene molecule. This electrostatic interaction is approximately ~30% more stable than the next conformer (1*trans*), where the halide bifurcates the C=C bond. Additional structures are also present in the bromide and chloride complexes (denoted 4*trans*), where the halide appends to a hydrogen on the terminal carbon similarly to previously studied halide-formic acid complexes.<sup>[13]</sup> These structures exhibit similar bonding motifs to the halide-propene complexes, where the bidentate structure is again the most stable complex.<sup>[14]</sup>

Similarly each halide structure also shows trends in their complex dissociation energy ( $D_0$ ) values that correspond to previously studied halide-propene complexes, with the chloride complexes being the most stable and the iodide complexes being the least stable.<sup>[14]</sup> Comparing the two bidentate complexes in the halide-propene and halide-butadiene complexes, the larger hydrocarbon chain is more stable. This is attributed to the delocalisation of donated electron density in the diene such that the charge density gradients are constructive, whereas in the propene complex the induced dipoles contain destructive vector components.

For the *cis*-butadiene complexes, while none of the structures are determined to be minima, the complexes are still stabilised compared to the monomer units. For the four structures present, each exhibit the same bonding motifs as their *trans* counterparts; either bifurcating a CC bond, bidentate coordination, or appending to a terminal hydrogen. Comparing the imaginary mode representing the rotation around the C–C bond in each of the complexes (in this case the  $\text{Cl}^-$  complexes) with that of the monomer ( $182i \text{ cm}^{-1}$ ), the 1*cis* ( $163i \text{ cm}^{-1}$ ), 2*cis* ( $171i \text{ cm}^{-1}$ ) and 5*cis* ( $139i \text{ cm}^{-1}$ ) structures do not significantly stabilise the rotation. The 2*cis* structure however has a frequency of  $49i \text{ cm}^{-1}$ , as the two coordinating hydrogens lie on either side of the C–C bond and as such the complex formation stabilises the rotation. While still an imaginary mode for each of the halides studied here, an anion with higher charge density such as fluoride may yield a stabilised *cis*-butadiene complex.

In the neutral complexes, each of the vdW complexes exhibit similar  $D_0$  values to comparative halide-propene complexes.<sup>[14]</sup> The most stable neutral complexes are the 7*cis* and 7*trans* structures respectively, as the halogen exhibits similar interaction with the  $\pi$ -system as the halogen-propene complexes. Despite the increase in complex stability in these cases, the 7*cis* structure still retains the imaginary mode ( $132i \text{ cm}^{-1}$ ) and it is not significantly stabilised with respect to the butadiene monomer. The 7*trans* structure however is reminiscent of the pre-reaction adduct in radical activation of butadiene by bromine to produce peroxy radicals, as reported in the literature.<sup>[9]</sup> In both cases similarly to the inversion of halide/halogen stability in the propene complexes, the halogen-butadiene complexes are less stable than the corresponding propene complexes. This is likely due to a combination of delocalisation through the carbon chain reducing the bonding interaction at any given carbon.

### Time-Of-Flight Mass Spectrometry

The mass spectra for the  $\text{CCl}_4$ ,  $\text{CH}_2\text{Br}_2$  and  $\text{CH}_3\text{I}$  gas mixtures are presented in Figures 2, 3 and 4. The mass spectra often contain residual halide sources from preceding gas mixtures. In this suite of experiments, the chronological order of experiments are those with  $\text{CH}_3\text{I}$ ,  $\text{CH}_2\text{Br}_2$  and finally  $\text{CCl}_4$ . This was done to ensure that either residual  $\text{Br}^-$  or  $\text{I}^-$  would be present in the  $\text{CCl}_4$  gas mixture for photoelectron spectroscopy (PES) calibration. Each of the mass spectra were calibrated against the bare halide peaks present in each, which were themselves identified

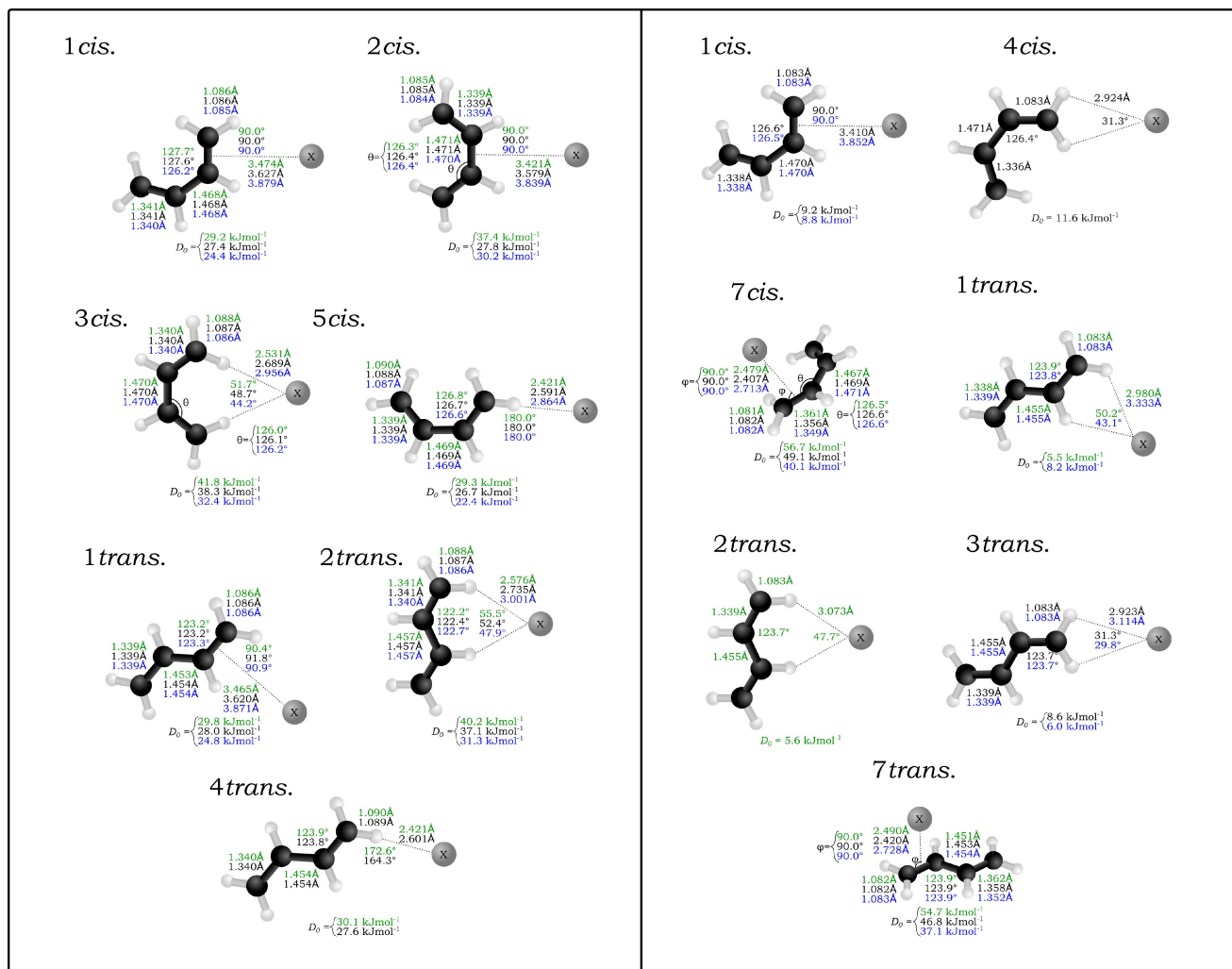


**Figure 1.** Optimised structures of the  $X\cdots C_4H_6$  anion (left) and neutral (right) complexes. Each structure is labelled based on the starting geometry described in Figure 11. Structures are calculated with the DSD-PBEP86-D3BJ functional with AVTZ basis sets, with structural differences for the chloride (green), bromide (black) and iodide (blue) complexes. Associated  $D_0$  values are included for each structure.

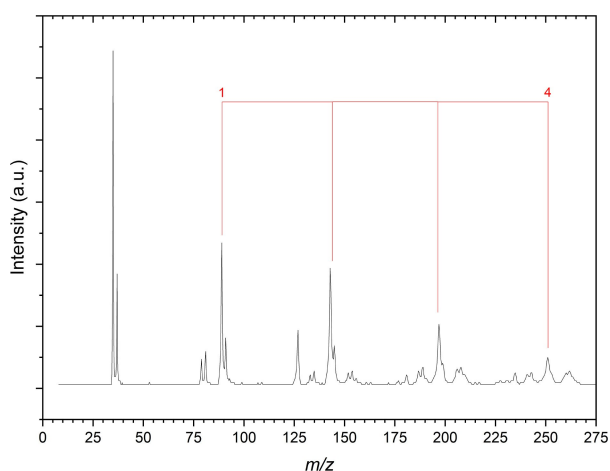


**Figure 2.** Time-of-flight mass spectrum produced from a  $CCl_4:C_4H_6:Ar$  gas mixture (trace:50 kPa:400 kPa). The spectrum features a number of the desired  $Cl^- \cdots (C_4H_6)_n$  complexes for  $n \leq 4$ , labelled by the red drop downs.

by their relative intensities and isotopic abundances. Full mass assignments are provided in Supplementary Information. For those mass peaks that are assigned to highly solvated complexes, given that each of the mass spectra are calibrated against peaks at comparatively low  $m/z$  values, uncertainty of the calibration may effect the absolute  $m/z$  values for these complexes. However as solvation occurs in a stepwise fashion, the separation and relative intensities of peaks within bands of the mass spectrum can be assigned with respect to neighbouring bands. By commencing assignments at low, well-defined  $m/z$  values and proceeding in series, full assignment of the spectrum is then achieved.

The mass spectrum of the  $CCl_4:C_4H_6:Ar$  gas mixture is shown in Figure 2. The spectrum shows clear mass peaks for the  $^{35,37}Cl^-$ ,  $^{79,81}Br^-$  and  $^{127}I^-$  ions. The spectrum also features a progression, marked by the red drop downs, of the  $^{35,37}Cl^- \cdots (C_4H_6)_n$  ( $n=1-4$ ) complexes. These peaks are identified based upon the isotopic abundances of the underlying chloride ion and, at higher  $m/z$  values, the relative  $\Delta m/z$  equal to the

mass of a single butadiene unit. The highest of these ( $\sim 250$   $m/z$ ), is no longer well resolved when compared to the bare chloride. This effect is the result of the relative time-of-flight (TOF) plate voltages and adjustment of the relative space focussing of the molecular beam. While this may be improved upon by adjusting the voltage applied to the front TOF plate, for the purposes of these photoelectron spectroscopy experiments optimum mass resolved isotopes of the same species are not paramount. Immediately preceding each of the  $^{35,37}\text{Cl}^-\dots(\text{C}_4\text{H}_6)_n$ , there are a number of spectral features that can be assigned to the respective butadiene solvated bromide complexes (for  $n=1-3$ ). The formation of these complexes is encouraging for later scheduled experiments, as are both peaks at 181 and 235  $m/z$  which represent  $\text{I}^-\dots(\text{C}_4\text{H}_6)_n$  for  $n \leq 2$ . Immediately following the chloride-butadiene complexes (from  $n=2$ ), a number of  $\text{Cl}^-\dots(\text{CCl}_3)(\text{C}_4\text{H}_6)_n$  complexes with up to two butadiene molecules are present. PES spectra were not recorded of these peaks to confirm their structure though they do present interesting opportunities for future work in investigating a mixed solvent, gas-phase complex.

The mass spectrum from the  $\text{CH}_2\text{Br}_2:\text{C}_4\text{H}_6:\text{Ar}$  gas mixture (Figure 3), shows good complex formation for a number of solvated bromide and iodide clusters. The space focussing of the time-of-flight photoelectron spectroscopy (TOF-PES) results in poorer mass resolution for  $>275$   $m/z$ , however the same approach that was used to analyse the  $\text{CCl}_4$  spectrum can be taken here. There are two progressions of solvated bromide complexes denoted in Figure 3 by red and blue drop downs. The peaks indicated in red represent the  $\text{Br}^-\dots(\text{C}_4\text{H}_6)_n$  ( $n=1-5$ ) complexes and starting at 133  $m/z$  with the monosolvated  $^{79}\text{Br}^-$  complex. The blue peaks start at 173  $m/z$  for  $n=0$  in a series of  $^{79,81}\text{Br}^-\dots(\text{CH}_2^{81,79}\text{Br})(\text{C}_4\text{H}_6)_n$  complexes. The bromide-bromomethyl radical peak has previously been studied by anion PES however as with the  $\text{Cl}^-\dots(\text{CCl}_3)$  complexes, the butadiene

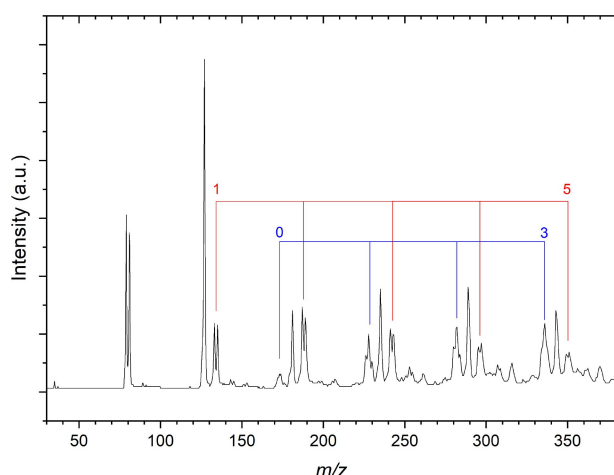


**Figure 3.** Time-of-flight mass spectrum produced from a  $\text{CH}_2\text{Br}_2:\text{C}_4\text{H}_6:\text{Ar}$  gas mixture (trace:50 kPa:400 kPa). The spectrum features a number of the desired  $\text{Br}^-\dots(\text{C}_4\text{H}_6)_n$  complexes for  $n \leq 5$ , labelled by the red drop downs, as well as peaks attributed to  $\text{Br}^-\dots(\text{CH}_2\text{Br})(\text{C}_4\text{H}_6)_n$  ( $n=0-3$ ) complexes (blue drop downs).

solvated complexes offer an opportunity to study solvation in a competitive environment.<sup>[15]</sup>

Particularly in these bromide-bromomethyl radical complexes, the relative intensities of the features in the mass spectrum increase with increasing butadiene solvation. This is believed to be a kinetic effect with a stark pressure dependence. The typical operating voltage of the piezo nozzle is  $\sim 340$  V, with increases in the applied voltage required throughout a day of experiments as the background pressure slowly increases. However it was found in these butadiene experiments that the mass spectrum intensities comparing high and low  $m/z$  peaks was greatly dependant on the nozzle voltage. At low voltages, low  $m/z$  peaks such as the bare halides and monosolvated halides produced good mass spectrum intensities whereas increases in the nozzle voltage of up to 10 V reduced these intensities as the high  $m/z$  peaks became more intense. This suggests that in the source chamber the amount of halide anions produced by dissociative electron attachment becomes rate limiting as the increased local partial pressure of butadiene and the halomethane source readily solvate the anion and anion complexes.

Lastly, the mass spectrum of the  $\text{CH}_3\text{I}:\text{C}_4\text{H}_6:\text{Ar}$  gas mixture is presented in Figure 4. The range of this spectrum is significantly larger than that of the corresponding bromide spectrum, with the largest spectral features recorded at 702  $m/z$ . As with the previous mass spectra, the  $\text{CH}_3\text{I}$  spectrum consists of a number of solvated iodide-butadiene complexes as well as mixed-solvent complexes. These are shown in Figure 4 as red, blue and orange drop downs which represent  $\text{I}^-\dots(\text{C}_4\text{H}_6)_n$  ( $n=1-10$ ),  $\text{I}^-\dots(\text{CH}_3\text{I})(\text{C}_4\text{H}_6)_n$  ( $n=0-8$ ) and  $\text{I}^-\dots(\text{CH}_3\text{I})_2(\text{C}_4\text{H}_6)_n$  ( $n=0-5$ ) respectively. As with the mixed-solvent bromide complexes, the nozzle voltage appears to affect the relative intensities of the peaks within each band, with the most intense comprising the  $n=3$  complex in each case. The strong iodide mass peak in Figure 3 coupled with the strong solvation progression present

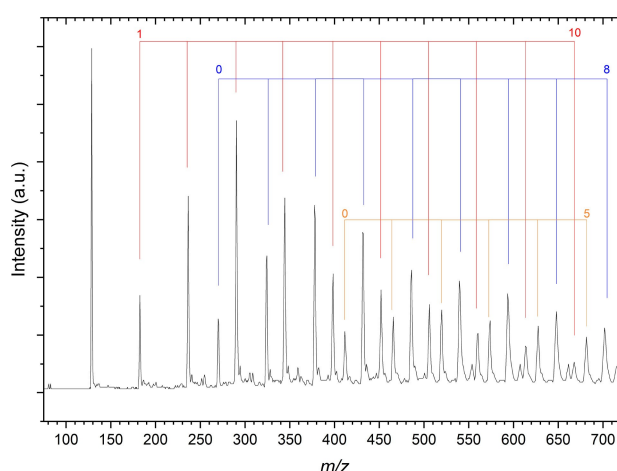


**Figure 4.** Time-of-flight mass spectrum produced from a  $\text{CH}_3\text{I}:\text{C}_4\text{H}_6:\text{Ar}$  gas mixture (trace:50 kPa:400 kPa). The spectrum features a number of the desired  $\text{I}^-\dots(\text{C}_4\text{H}_6)_n$  complexes for  $n \leq 10$ , labelled by the red drop downs, as well as peaks attributed to  $\text{I}^-\dots(\text{CH}_3\text{I})(\text{C}_4\text{H}_6)_n$  ( $n=0-8$ ) complexes (blue drop downs) and  $\text{I}^-\dots(\text{CH}_3\text{I})_2(\text{C}_4\text{H}_6)_n$  ( $n=0-8$ ) complexes (orange drop downs).

in the  $\text{CH}_3\text{I}$  mass spectrum is indicative of the relatively large amount of  $\text{CH}_3\text{I}$  present in this gas mix.

At high  $m/z$ , the spectrum becomes increasingly congested as the number of permutations of the monomer units grows. In order to perform PES spectroscopy on peaks in this region, similarly to their mass assignment, the Q-switch timing of the Nd:YAG laser may be correlated against the ion TOF and used to predict Q-switch timings that intersect these larger clusters. This is especially useful in performing spectroscopy on peaks where the mass spectrum is less intense and the contained anion complexes produce photoelectrons with TOF similar to those of the background ion noise.

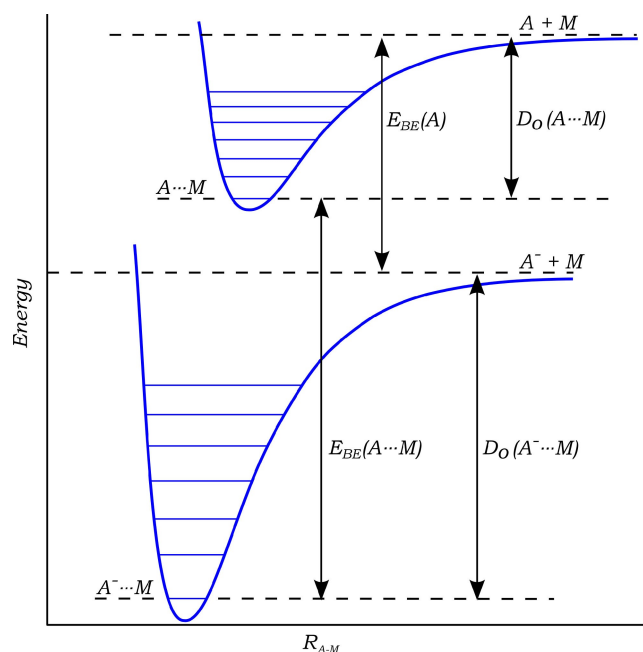


**Figure 5.** Illustrative anion and neutral potential energy surfaces of A solvated by M.  $E_{BE}$  values are the electron binding energies of the complex and bare A, and  $D_0$  are the respective complex stabilisation energies of the anion and neutral complexes. Note that  $E_{BE}(A...M) + D_0(A...M) = E_{BE}(A) + D_0(A^-...M)$ , and  $E_{stab} = E_{BE}(A...M) - E_{BE}(A) = D_0(A^-...M) - D_0(A...M)$ . This can be extended for increasing solvation where  $E_{solv}(n) = E_{stab}(n) - E_{stab}(n-1)$ .

## Photoelectron Spectra

The photoelectron spectra of the  $\text{Cl}^- \cdots (\text{C}_4\text{H}_6)_n$   $n = 0-3$  complexes are presented in Figure 5. Each of the spectra are fitted with two Gaussian functions as per Equation 3. The determined electron binding energy ( $E_{BE}$ ) for each of the perturbed  $^2P_{3/2}$  peaks are then presented in Table 1. In each case, the degree of stabilisation gained through solvation is expressed as the increase in  $E_{BE}$  and is referred to as the electron stabilisation energy ( $E_{stab}$ ). This is illustrated in Figure 6. As there are multiply solvated halides present in these spectra, the stepwise solvation energy ( $E_{solv}$ ) is a measure of the successive electronic stabilisation ( $\Delta E_{stab}$ ) with each additional solvating molecule.

The  $E_{BE}$  of the  $\text{Cl}^- \cdots \text{C}_4\text{H}_6$  complex is determined from peak fitting as 3.9962(6) eV but is reported to 3 s.f. Comparing the experimental  $E_{BE}$  (4.00 eV) with the vertical detachment energies (VDE) calculated from DSD-PBEP86-D3BJ/AVTZ calculations, the most probable anion structure is again the *2trans* complex (4.02 eV). The *1trans* and *4trans* conformers are structurally similar and have similar  $D_0$  values, with corresponding VDE values of 3.88 eV and 3.93 eV respectively. Given the quality of the fit in this case ( $R^2 = 0.9826$ ), this is believed to be sufficiently different to assign the spectrum to the *2trans* structure. The  $E_{stab}$  of the complex is determined to be 39.0 kJ/mol which shows good agreement with the determined  $D_0$  of the anion complex. The calculated  $E_{stab}$  is 34.6 kJ mol $^{-1}$ , but represents the adiabatic detachment energy (ADE) rather than VDE. Extending this to the further solvated chloride-butadiene complexes, the  $E_{solv}$  show successive decreases with increasing degrees of solvation. These experimental  $E_{solv}$  energies are 27.6 kJ mol $^{-1}$  and 20.9 kJ mol $^{-1}$  respectively, indicating the stability in these anion complexes.

From the fitting of the experimental chloride-butadiene spectra, it is clear that the fitted Gaussian functions become narrower as the  $E_{BE}$  approaches the photon energy (i.e. low electron kinetic energy ( $E_{KE}$ )). Fitting a linear regression through this data of  $E_{KE}$  against  $\sigma$  for each fit yields the function  $\sigma = 9.7 \times 10^{-2} E_{KE} + 3.02 \times 10^{-2}$  ( $R^2 = 0.9821$ ) and provides some predictive power as to the expected Gaussian width of a given transition. The corresponding  $dE/E_{KE}$  values range from 30% to 64% near threshold.

The photoelectron spectra from the  $\text{Br}^- \cdots (\text{C}_4\text{H}_6)_n$  ( $n = 1-3$ ) complexes are presented in Figure 7. The  $E_{BE}$  of the  $n = 1$  complex is determined as 3.66 eV with a resulting  $E_{stab}$  of

**Table 1.** Comparison between the experimental electronic binding energy ( $E_{BE}$ ), stepwise solvation energy ( $E_{solv}$ ) and calculated VDE for the halide-butadiene complexes (all in eV).

$n$	$\text{Cl}^- \cdots (\text{C}_4\text{H}_6)_n$	$E_{BE}$	$VDE_{Calc}$	$E_{solv}$	$\text{Br}^- \cdots (\text{C}_4\text{H}_6)_n$	$E_{BE}$	$VDE_{Calc}$	$E_{solv}$	$\text{I}^- \cdots (\text{C}_4\text{H}_6)_n$	$E_{BE}$	$VDE_{Calc}$	$E_{solv}$
0		3.59				3.34				3.06		
1		4.00	4.02	0.40		3.66	3.70	0.31		3.27	3.31	0.21
2		4.28		0.29		3.91		0.26		3.47	3.52	0.20
3		4.50		0.22		4.13		0.21		3.64		0.17
4										3.78		0.14
5										3.93		0.15
6										4.06		0.13
7										4.27		0.21

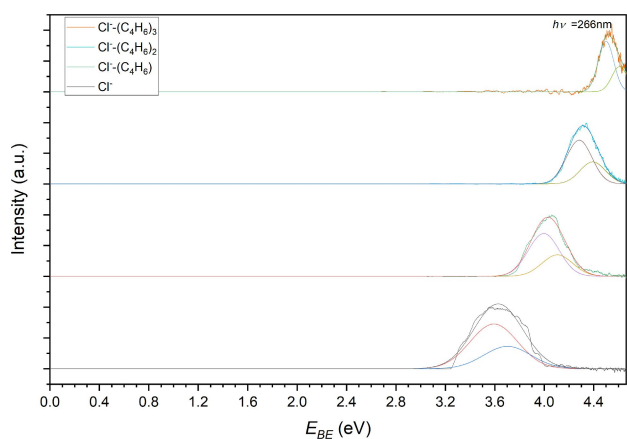


**Figure 6.** Photoelectron spectrum of  $\text{Cl}^- \cdots (\text{C}_4\text{H}_6)_n$  ( $n = 1-3$ ) complexes from Figure 2 assigned to photodetachment to the perturbed  $^2\text{P}_{3/2}$  and  $^2\text{P}_{1/2}$  states of each complex. Each complex is deconvoluted into two Gaussian functions representing the two  $^2\text{P}$  peaks.

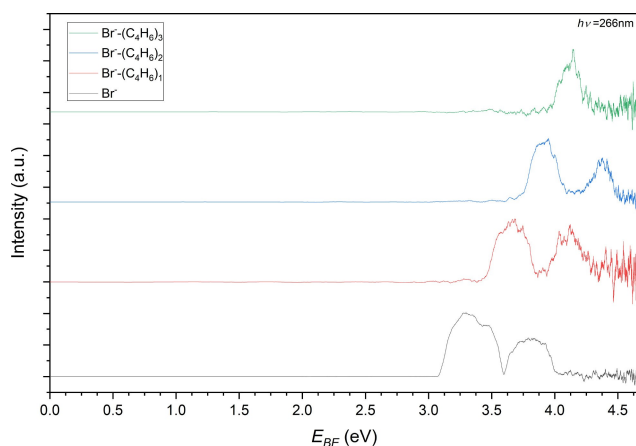


**Figure 7.** Photoelectron spectrum of  $\text{Br}^- \cdots (\text{C}_4\text{H}_6)_n$  ( $n = 0-3$ ) complexes from Figure 3 assigned to photodetachment to the perturbed  $^2\text{P}_{3/2}$  and  $^2\text{P}_{1/2}$  states of each complex.

0.31 eV (30.2 kJ mol<sup>-1</sup>). Compared to the chloride complexes, the  $\text{Br}^- \cdots \text{C}_4\text{H}_6$  calculated  $D_0$  value does not agree as well with the VDE. Considering that the neutral complexes are generally more strongly bound moving down the group 17 elements, this deviation away from alignment is attributed to the more appropriate definition of the difference in  $D_0$  values. This suggests that the VDE conformation in the neutral state is bound, albeit vibrationally excited. Of the neutral bromine vdW minima, the  $D_0$  values range from 8.6 kJ mol<sup>-1</sup> to 11.6 kJ mol<sup>-1</sup>. For the anion complexes, the *1trans* and *4trans* complexes have  $D_0$  values of 28.0 kJ mol<sup>-1</sup> and 27.6 kJ mol<sup>-1</sup> respectively. As these are both less than the  $E_{stab}$  energy it suggests that photodetachment from these complexes, while possible, would be to unbound states as only a negative  $D_0$  in the neutral would produce such an  $E_{stab}$ .

Photoelectron spectroscopy of the iodide-butadiene complexes were successfully performed for up to seven solvating butadiene molecules. This was helped by the larger spin-orbit

splitting of the neutral iodine, bringing the  $E_{BE}$  of the  $^2\text{P}_{3/2}$  peak for higher solvated complexes below that of the photon energy. These photoelectron spectra are presented in Figure 8 and the  $E_{BE}$  values of each peak presented in Table 1.

The  $E_{BE}$  of the perturbed  $^2\text{P}_{3/2}$  peak is 3.27 eV and the calculated  $E_{stab}$  of the monosolvated complex is 0.21 eV (20.4 kJ mol<sup>-1</sup>). Unlike the bromide complexes, the  $D_0$  values of both iodide complexes are greater than the  $E_{stab}$  from experiment and both possible photodetachment channels. As the *2trans* complex is significantly more stable and the neutral  $D_0$  values are ~8 kJ mol<sup>-1</sup>, it suggests that it is still the most probable anion structure as the resulting  $E_{stab}$  values are closest to experiment.

As there are a number of solvated structures present for each of the halides, it is necessary to consider whether butadiene [4 + 2] Diels-Alder cycloaddition occurs within the gas mixture. To investigate this, additional DSD-PBEP86-D3BJ calculations were performed on the iodide complex with the most probable product, 4-vinylcyclohexene. As the number of heavy atoms increased significantly in these larger complexes, the basis set used was the def2TZVPD. The def2 basis set was chosen here based on the reliability of the def2QZVPD basis set for troublesome cases.<sup>[14]</sup> These were compared with a minimum structure representing the  $\text{I}^- \cdots (\text{C}_4\text{H}_6)_2$  complex where the butadiene monomers interacted with the iodide similarly to the *2trans* conformer of the monosolvated complex. The results of these calculations are shown in Figure 9, where two minima and a transition state were determined for the 4-vinylhexene complex and one structure was determined for the trimer complex. The trimer structure is a transition state where the imaginary mode (53i cm<sup>-1</sup>) represents a rotation of the butadiene monomers such that their interaction is not directly towards the iodide. The proposed offset arrangement of the butadiene monomers does still represent a good approximation of the trimer structure. Undertaking VDE calculations of the two iodide-4-vinylhexene complexes and the  $\text{I}^- \cdots (\text{C}_4\text{H}_6)_2$  complexes yields distinct values of 3.19 eV, 3.35 eV and 3.52 eV respectively. The  $D_0$  values of the 4-vinylhexene complexes are also

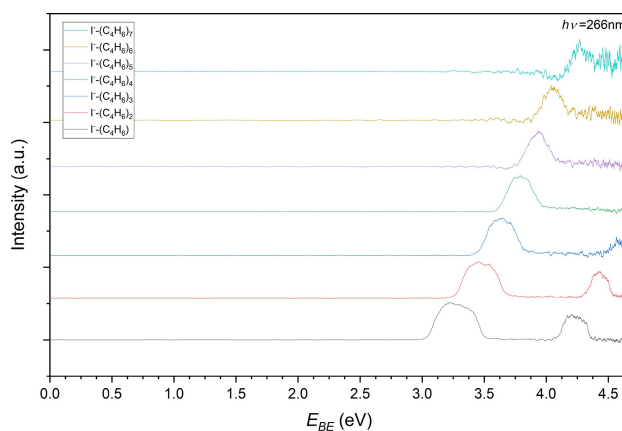


**Figure 8.** Photoelectron spectrum of  $\text{I}^- \cdots (\text{C}_4\text{H}_6)_n$  ( $n = 1-7$ ) complexes from Figure 4 assigned to photodetachment to the perturbed  $^2\text{P}_{3/2}$  and  $^2\text{P}_{1/2}$  states of each complex.

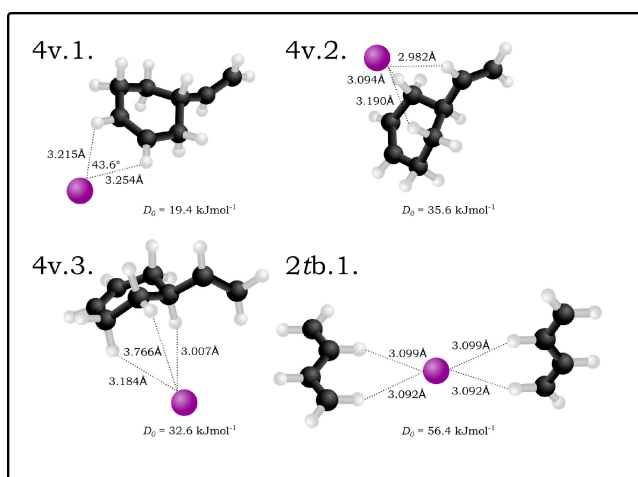


**Figure 9.** Optimised structures of the  $I^- \cdots C_8H_{12}$  and  $I^- \cdots (C_4H_6)_2$  anion complexes. Structures are calculated with the DSD-PBEP86-D3BJ functional with def-2QZVPD basis set. Associated  $D_0$  values are included for each structure.

similar to those of the monosolvated iodide-butadiene complex, indicating that the degree of stabilisation is more dependant on the degree of solvation than the solvent molecule in this case. Compared with the experimental detachment (3.47 eV), only the trimer complex agrees reasonably with the experimental perturbed  ${}^2P_{3/2}$  peak and thus the Diels-Alder product is subsequently ruled out from higher butadiene complexes for each halide.

In both the bromide and iodide complexes there is a similarly distinct decrease in the  $E_{solv}$  energy as there was in the chloride complexes. These energies are plotted against the number of solvating butadiene molecules, and compared with other larger halide clusters with  $H_2O$ ,  $CO_2$  and  $N_2O$  in literature in Figure 10.<sup>[16–18]</sup> As noted by Markovich in comparing halide-water clusters, the  $E_{solv}$  energy decreases with each successive solvent molecule until a full solvation shell is filled. The onset of solvating molecules filling a second solvation shell is marked by a sharp increase in the  $E_{solv}$  for that number of molecules. In the case of the iodide-butadiene clusters this occurs at  $n = 7$  and is indicative that the filled first solvation shell consists of six coordinated butadiene molecules. The  $E_{solv}$  for  $n = 7$  is approximately equal to that of the monosolvated complex suggesting that the filling of the second solvation shell treats the complete first shell as a single core, much like a bare iodide albeit shielded. Interestingly there is also present at  $n = 5$  a small increase in the  $E_{solv}$  which suggests that the 4-coordinated complex may itself be a metastable structure. Conversely however, photoelectron spectra of  $IO_3^- \cdots (H_2O)_n$  show a marked decrease in  $\Delta E_{BE}$  (here  $E_{solv}$ ) at  $n = 10$ .<sup>[19]</sup> Here the change in stabilisation was attributed asymmetric solvation where stable anion geometries correspond to higher energy conformers in the neutral state. Considering this, and without calculated geometries for the highly solvated  $I^- \cdots (C_4H_6)_n$  anion and neutral complexes, determination of the solvation shell is inconclusive and further studies would be required.

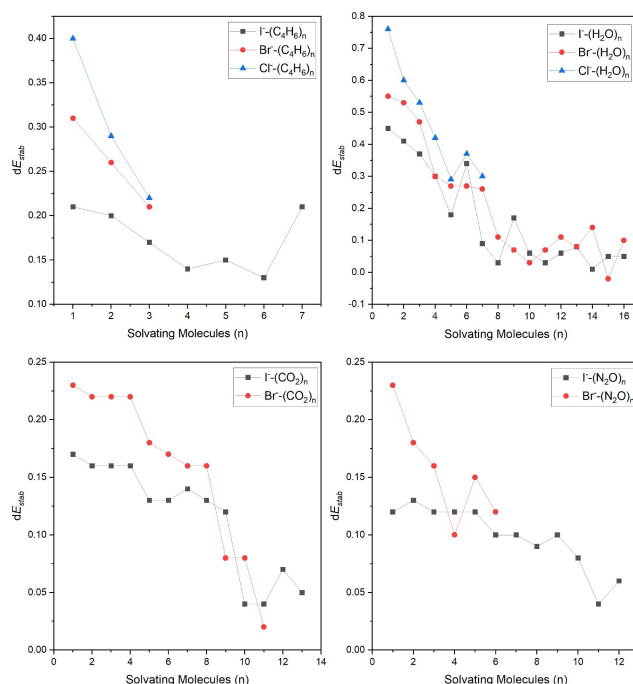


**Figure 10.** Comparison of trends in  $E_{solv}$  for a range of solvated halide complexes with butadiene,  $H_2O$ ,<sup>[18]</sup>  $CO_2$ ,<sup>[17]</sup> and  $N_2O$ .<sup>[16,17]</sup>

## Conclusion

In summary, a number of  $X^- \cdots (C_4H_6)_n$  ( $X = Cl, Br, I$ ;  $n \leq 3, 3, 7$  respectively) complexes have been formed in the gas-phase and their anion photoelectron spectra recorded. To complement these experimental results the structures of several vdW complexes have been calculated for each of the halide and halogen species with both *cis*- and *trans*-1,3-butadiene using the DSD-PBEP86-D3BJ functional. For the monosolvated complexes, the  $E_{stab}$  values decrease as the size of halide increases and from calculation are most stable when coordinated by bidentate hydrogens from the butadiene. The VDE of these complexes was determined as 4.00 eV, 3.66 eV and 3.27 eV for the  $Cl^-$ ,  $Br^-$  and  $I^-$  complexes respectively. The difference in stabilisation trend with respect to the halide decreases as the number of solvating butadiene molecules increases with  $n = 3$  near parity.

As the 1,3-butadiene may undergo a [4+2] cycloaddition, the iodide complex of the product 4-vinylcyclohexene was also calculated. The VDE of this complex was found to be 3.35 eV whereas the trimer butadiene complex has a VDE of 3.52 eV, much more aligned to the experimental value of 3.47 eV.

Within the solvation of the iodide-butadiene complexes, the stepwise solvation energy generally decreases with the number of solvating butadiene molecules. There are two points where the solvation energy increases at  $n = 5$  and  $n = 7$  which may indicate that the  $n = 4$  represents a metastable solvated iodide and the  $n = 6$  represents a full solvation shell.

## Experimental

### Experimental Methods

All experiments were conducted using a TOF-PES spectrometer that has been detailed previously and only relevant details are included here.<sup>[20,21]</sup> Gas mixtures were prepared by introduction of the relevant halide source ( $\text{CCl}_4$ ,  $\text{CH}_2\text{Br}_2$  and  $\text{CH}_3\text{I}$ ) followed by a partial pressure of 1,3-butadiene (*Sigma-Aldrich* > 99%, 100 g) and then made up to operational pressure (450 kPa). When preparing the gas mixtures, lab lighting was switched off to reduce any potential light-activated cycloadditions in the line of the gas mixing station. The clear Teflon gas line that connected the gas mixing station to the piezo nozzle assembly was then also covered in aluminium foil. The original gas mixture, consisting of  $\text{CH}_3\text{I}:\text{C}_4\text{H}_6:\text{Ar}$  was made with trace methyl iodide and a partial pressure of 30 kPa of 1,3-butadiene. This however did not yield significant intensities in the mass spectrum to perform PES and the gas mixture was remade with a higher partial pressure of 50 kPa. The improved intensities in the mass spectrum informed the later  $\text{CH}_2\text{Br}_2$  and  $\text{CCl}_4$  gas mixtures and this partial pressure of 1,3-butadiene remained unchanged.

In attempting to form larger clusters the beam energy was increased to  $-2200$  V for the  $\text{CH}_3\text{I}$  gas mixture to improve the beam stability and reduce the influence of stray fields. While this broadened the peaks presented, the associated reduction in energy resolution was acceptable to form highly solvated 1,3-butadiene complexes as the spin-orbit splitting of the  $^2P$  states of iodine is greatest of the selected halides. For the corresponding  $\text{Br}^-$  and  $\text{Cl}^-$  spectra, the beam energy was reduced to  $-1500$  V to adequately resolve the  $^2P$  peaks and reduce the width of fitted Gaussian functions respectively. The timescale of the experiment is such that the voltage is applied to the TOF plates at  $T_{0+}404.34$   $\mu\text{s}$  and the laser is Q-switched at  $+22.91$   $\mu\text{s}$  relative to the TOF plates to intersect the laser pulse with  $\text{I}^-$  in the ion beam. This was particularly important for larger  $\text{I}^-\cdots(\text{C}_4\text{H}_6)_n$  complexes as the correlation between the Q-switch timing and the ion TOF was used to guide temporal photodetachment searches.

PES spectra were analysed in two different approaches. For the  $\text{Br}^-$  and  $\text{I}^-$  PES spectra, where the  $^2P$  peaks are resolved, the peak positions are determined by averaging the ebe values at half-maximum intensity for each peak. For the  $\text{Cl}^-$  spectra, the peak positions are determined by fitting a pair of Gaussian functions as per Equation 3.<sup>[22]</sup>

$$I = Ae^{-\frac{(E_{\text{BE}} - \text{VDE})^2}{2\sigma^2}} + \frac{1}{2}Ae^{-\frac{(E_{\text{BE}} - \text{VDE} - 0.109)^2}{2\sigma^2}} \quad (3)$$

### Computational Methods

The DSD-PBEP86-D3BJ double-hybrid functional with def2QZVP and aug-cc-pVTZ (denoted AVTZ) basis sets was used to perform a conformer search for both the *cis*- and *trans*-1,3-butadiene halide and halogen complexes.<sup>[23–27]</sup> The DSD-PBEP86-D3BJ functional was chosen for its efficacy in describing long-range interactions and applicability to similar systems previously.<sup>[14,28]</sup> For Cl additional diffuse functions are included and for Br and I, effective core potentials are included for the AVTZ basis set.<sup>[29,30]</sup> Starting geometries utilised a number of different bonding arrangements with respect to the double bonds of the butadiene molecules similarly to previously studied ethene and propene complexes.<sup>[14,31]</sup> These included where the halide or halogen bifurcates the C=C or C–C bond, is bidentate coordinated by the butadiene, appends to a single hydrogen or is bound out-of-plane from the butadiene. Due

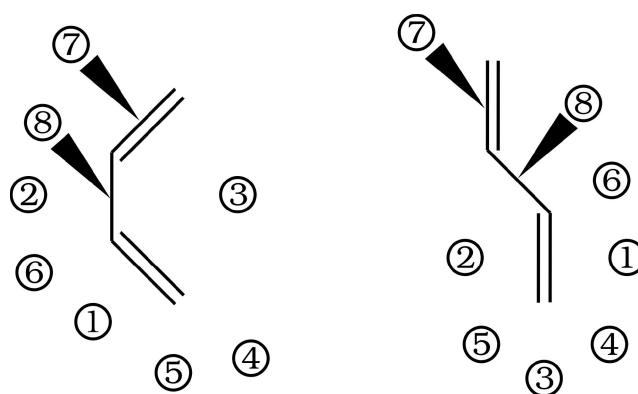


**Figure 11.** Starting geometries for the  $\text{X}\cdots\text{C}_4\text{H}_6$  complexes. Each structure referred to in text is numbered by the location of the halide/halogen for both the *cis* (left) and *trans* (right) isomers.[fig.xbutasearch]

to the number of these conformers each is numbered for *cis*- and *trans*-1,3-butadiene as per Figure 11 and referred to in text as such. The starting geometries are generally numbered with an order representing the bifurcation of a bond or bisection of an angle, followed by hydrogen-appended geometries, followed by out-of-plane interactions with a bond.

All structures were screened by harmonic frequency calculations using the associated basis set of their optimisation using Gaussian 09.<sup>[32]</sup> For the *trans*-1,3-butadiene complexes, conformers were screened to be minima, however the *cis*-1,3-butadiene monomer is itself a transition state where the imaginary mode represents a rotation around the C–C bond. For these complexes, while  $D_0$  values are also reported as they provide an indication as to the relative stability of the complexes, the reduction in the imaginary mode compared to the monomer is also considered. Similar protocols to those used previously for the determination of vdes of the respective complexes was then undertaken, with only halide-*trans*-butadiene complexes considered.<sup>[14]</sup>

### Acknowledgements

This research was undertaken with the assistance of computational resources from the Pople high-performance computing cluster of the Faculty of Science at the University of Western Australia. The Australian Research Council is acknowledged for funding the laser installation under the LIEF scheme (LE110100093). The School of Molecular Sciences and the Faculty of Science are acknowledged for financial support. T.R.C. and H.T.R. thank the support of Research Training Program (RTP) scholarships funded by the Australian Government, C.T.H. acknowledges the UWA Dean's Excellence in Science PhD Scholarship, and P.D.W. thanks the support of the Center for Materials Crystallography at Aarhus University in Denmark, funded by the Danish National Research Foundation (DNRF93). Open Access publishing facilitated by The University of Western Australia, as part of the Wiley - The University of Western Australia agreement via the Council of Australian University Librarians.

## Conflict of Interests

The authors declare no conflict of interest.

## Data Availability Statement

The data that support the findings of this study are available from the corresponding author upon reasonable request.

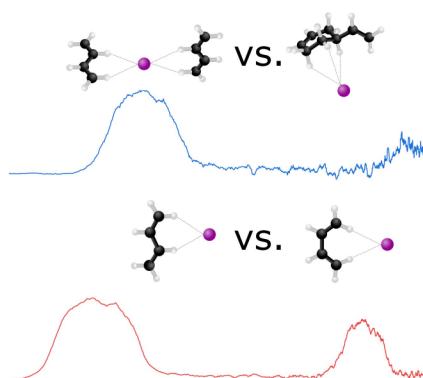
**Keywords:** gas-phase solvation · photoelectron spectroscopy · noncovalent interactions · butadiene · interstellar medium

- [1] M. J. Abplanalp, S. Gabi, R. I. Kaiser, *Phys. Chem. Chem. Phys.* **2019**, *21*, 5378–5393.
- [2] B. M. Jones, F. Zhang, R. I. Kaiser, A. Jamal, A. M. Mebel, M. A. Cordiner, S. B. Charnley, *Proc. Natl. Acad. Sci. USA* **2010**, *108*, 452–457.
- [3] S. B. Morales, C. J. Bennett, S. D. Le Picard, A. Canosa, I. R. Sims, B. J. Sun, P. H. Chen, A. H. H. Chang, V. V. Kislov, A. M. Mebel, et al., *The Astrophysical Journal* **2011**, *742*, 26.
- [4] L. G. Muzangwa, T. Yang, D. S. N. Parker, R. I. Kaiser, A. M. Mebel, A. Jamal, M. Ryazantsev, K. Morokuma, *Phys. Chem. Chem. Phys.* **2015**, *17*, 7699–7706.
- [5] R. I. Kaiser, D. S. N. Parker, F. Zhang, A. Landera, V. V. Kislov, A. M. Mebel, *J. Phys. Chem. A* **2012**, *116*, 4248–4258.
- [6] K. Chenoweth, A. C. T. van Duin, S. Dasgupta, W. A. Goddard III, *J. Phys. Chem. A* **2009**, *113*, 1740–1746.
- [7] S. Vijayakumar, B. Rajakumar, *J. Phys. Chem. A* **2017**, *121*, 1976–1984.
- [8] N. Hansen, J. A. Miller, T. Kasper, K. Kohse-Höinghaus, P. R. Westmoreland, J. Wang, T. A. Cool, *Proc. Combust. Inst.* **2009**, *32*, 623–630.
- [9] P. L. Laine, Y. S. Sohn, J. M. Nicovich, M. L. Mc-Kee, P. H. Wine, *J. Phys. Chem. A* **2012**, *116*, 6341–6357.
- [10] K. Hiraoka, S. Mizuse, S. Yamabe, *J. Phys. Chem.* **1988**, *92*, 3943–3952.
- [11] W. v. E. Doering, M. Franck-Neumann, D. Hasselmann, R. L. Kaye, *J. Am. Chem. Soc.* **1972**, *94*, 3833–3844.
- [12] W. J. Lording, T. Fallon, M. S. Sherburn, M. N. Paddon-Row, *Chem. Sci.* **2020**, *11*, 11915–11926.
- [13] C. T. Haakansson, T. R. Corkish, P. D. Watson, H. T. Robinson, J. R. Brookes, H. C. Adam, A. J. McKinley, D. A. Wild, *Phys. Chem. Chem. Phys.* **2022**, *24*, 24748.
- [14] P. D. Watson, T. R. Corkish, C. T. Haakansson, A. J. McKinley, D. A. Wild, *Phys. Chem. Chem. Phys.* **2022**, *24*, 25842.
- [15] C. T. Haakansson, T. R. Corkish, P. D. Watson, A. J. McKinley, D. A. Wild, *Chem. Phys. Lett.* **2020**, *761*, 138060.
- [16] K. Lapere, Anion Photoelectron Spectroscopy of Halide Complexes and Clusters, Ph.D. thesis, University of Western Australia: School of Chemistry and Biochemistry **2015**.
- [17] D. W. Arnold, S. E. Bradforth, E. H. Kim, D. M. Neumark, *J. Chem. Phys.* **1995**, *102*, 3510–3518.
- [18] G. Markovich, S. Pollack, R. Giniger, O. Cheshnovsky, *J. Chem. Phys.* **1994**, *101*, 9344–9353.
- [19] H. Wen, G.-L. Hou, S. M. Kathmann, M. Valiev, X.-B. Wang, *J. Chem. Phys.* **2013**, *138*, 031101.
- [20] K. Lapere, R. LaMacchia, L. Quak, A. McKinley, D. Wild, *Chem. Phys. Lett.* **2011**, *504*, 13.
- [21] T. R. Corkish, C. T. Haakansson, P. D. Watson, A. J. McKinley, D. A. Wild, *ChemPhysChem* **2020**, *22*, 69–75.
- [22] P. D. Watson, H.-w. Yong, K. M. Lapere, M. Kettner, A. J. McKinley, D. A. Wild, *Chem. Phys. Lett.* **2016**, *654*, 119.
- [23] S. Kozuch, J. M. L. Martin, *Phys. Chem. Chem. Phys.* **2011**, *13*, 20104.
- [24] S. Kozuch, J. M. L. Martin, *J. Comput. Chem.* **2013**, *34*, 2327.
- [25] F. Weigend, R. Ahlrichs, *Phys. Chem. Chem. Phys.* **2005**, *7*, 3297.
- [26] F. Weigend, *Phys. Chem. Chem. Phys.* **2006**, *8*, 1057.
- [27] T. H. Dunning, K. A. Peterson, A. K. Wilson, *J. Chem. Phys.* **2001**, *114*, 9244.
- [28] T. R. Corkish, C. T. Haakansson, P. D. Watson, H. T. Robinson, A. J. McKinley, D. A. Wild, *ChemPhysChem* **2021**, *22*, 1316–1320.
- [29] K. A. Peterson, D. Figgen, E. Goll, H. Stoll, M. Dolg, *J. Chem. Phys.* **2003**, *119*, 11113.
- [30] K. A. Peterson, B. C. Shepler, D. Figgen, H. Stoll, *J. Phys. Chem. A* **2006**, *110*, 13877.
- [31] C. T. Haakansson, T. R. Corkish, P. D. Watson, D. B. 't Hart, A. J. McKinley, D. A. Wild, *Chem. Phys. Lett.* **2022**, *793*, 139433.
- [32] M. J. Frisch, G. W. Trucks, H. B. Schlegel, G. E. Scuseria, M. A. Robb, J. R. Cheeseman, G. Scalmani, V. Barone, B. Mennucci, G. A. Petersson, H. Nakatsuji, M. Caricato, X. Li, H. P. Hratchian, J. Izmaylov, A. F.; Bloino, G. Zheng, J. L. Sonnenberg, M. Hada, M. Ehara, K. Toyota, R. Fukuda, J. Hasegawa, M. Ishida, T. Nakajima, Y. Honda, O. Kitao, H. Nakai, T. Vreven, J. Montgomery, J. A., J. E. Peralta, F. Ogliaro, M. Bearpark, J. J. Heyd, E. Brothers, K. N. Kudin, V. N. Staroverov, R. Kobayashi, J. Normand, K. Raghavachari, A. Rendell, J. C. Burant, S. S. Iyengar, J. Tomasi, M. Cossi, N. Rega, M. J. Millam, M. Klene, J. E. Knox, J. B. Cross, V. Bakken, C. Adamo, J. Jaramillo, R. Gomperts, R. E. Stratmann, O. Yazyev, A. J. Austin, R. Cammi, C. Pomelli, J. W. Ochterski, R. L. Martin, K. Morokuma, V. G. Zakrzewski, G. A. Voth, P. Salvador, J. J. Dannenberg, S. Dapprich, A. D. Daniels, O. Farkas, J. B. Foresman, J. V. Ortiz, J. Cioslowski, D. J. Fox, Gaussian 09 Revision D.01, Gaussian Inc. Wallingford CT **2009**.

Manuscript received: November 16, 2022  
Accepted manuscript online: February 16, 2023  
Version of record online: ■■■, ■■■

## RESEARCH ARTICLE

Photoelectron spectra for  $X^{\ominus} \cdots (C_4H_6)_n$  ( $X = Cl, Br, I$  and  $n = 1-3, 1-3$  and  $1-7$  respectively) are presented. For all complexes, the calculated structures indicate that butadiene is bound in a bidentate fashion through H-bonding, with the Cl complex showing the greatest degree of stabilisation of the internal C–C rotation of *cis*-butadiene. These results have implications for gas-phase clustering in atmospheric and extraterrestrial environments.



*P. D. Watson, C. T. Haakansson, H. T. Robinson, T. R. Corkish, J. R. Brookes, Prof. A. J. McKinley, Dr. D. A. Wild\**

1 – 10

**Closing the Shell: Gas-Phase Solvation of Halides by 1,3-Butadiene**

